

Contents lists available at ScienceDirect

Simulation Modelling Practice and Theory

journal homepage: www.elsevier.com/locate/simpat





Hybrid simulation to support interdependence modeling of a multimodal transportation network

José Azucena, Basem Alkhaleel, Haitao Liao*, Heather Nachtmann

Department of Industrial Engineering, University of Arkansas, Fayetteville, AR 72701, USA

ARTICLE INFO

Keywords: Spatio-temporal statistics Inland waterways Interdependence modeling Agent-based simulation NetLogo

ABSTRACT

The inland waterways in the United States (U.S.) transport approximately 20% of coal, 22% of petroleum products, and 60% of farm exports making these waterways a significant contributor to the U.S. multimodal transportation system. In this study, data of extreme natural events affecting the U.S. inland waterways are collected and used to predict possible occurrences of such events using a spatio-temporal statistical model. A simulation tool incorporating this model is developed to investigate the impact of waterway disruptions on the interconnected multimodal transportation systems. A case study on the lower Mississippi River and the McClellan–Kerr Arkansas River Navigation System along with the related highways is provided to illustrate the use of the simulation tool for operation simulation and interdependence modeling of the multimodal transportation network. This tool provides a flexible means for quickly evaluating the performance of such Interdependent Critical Infrastructures (ICIs) and assisting in decision making.

1. Introduction

1.1. Background and motivation

The physical distribution infrastructure is critical to national security, economic well-being, global competitiveness, and quality of life in the United States (U.S.) [1]. The distribution infrastructure, referred to as the transportation network, includes but is not limited to the interconnected network of ports, inland waterways, highways, and railroads. The U.S. transportation network comprises almost 4 million miles (6.43 million kilometers) of public roads and highways, more than 360,000 interstate trucking companies and 20 million trucks for business, and 1900 seaports and 1700 inland river terminals on 11,000 miles of inland waterways carrying grain, chemicals, petroleum products, and import and export goods [2–4].

Many industries rely on the U.S. transportation network; thus, the economic impacts of disruptions affecting the network are expected to be substantial. Such interruptions can cause a cascading effect that can become widespread due to the spatial and temporal distributions of commodity flows [5]. Even without large-scale disruptions, the Federal Highway Administration (FHWA) estimated the trucking industry losses to be around \$8 billion a year due to highway congestion [5,6]. Such losses are expected to increase in the future due to forecasted increases in the U.S. domestic freight tonnages by approximately 50% in the next fifteen years [4,7,8]. In addition to highway network impacts, railways are expected to experience more significant congestions and breakdowns due to increased demand for Class I railroads [9].

The U.S. Maritime Administration, an agency of the U.S. Department of Transportation, has called for investment in the domestic waterways for freight movement [10], recognizing the need to reduce road and rail congestion. The increased use of 25,000 miles

E-mail address: liao@uark.edu (H. Liao).

^{*} Corresponding author.

of inland waterway freight transport could result in less congestion on U.S. roads and a reduction in the risk of road and rail transport accidents and possibly even reduce emissions of air pollution [5]. Barge transport is frequently cheaper than rail and truck alternatives, and there are many products which are too large for other transport methods. In 2017, the U.S. inland waterways were used to transport approximately 20% of America's coal, 22% of U.S. petroleum products, and 60% of farm exports between 38 states summing up the annual weight transported to around 630 million tons [3,4].

Although general freight movements via the inland waterways are expected to increase in the upcoming years due to economic and logistic drivers, research investigating the impacts of disruptions on waterway operations, multimodal commodity flow, and economic analysis are limited. Indeed, one reason for the limited number of studies may be the lack of tools that could facilitate research in this area by providing data-driven models. There is an urgent need to protect and coordinate U.S. multimodal transportation infrastructure to support strong economic growth and national security. Inland waterways and road and rail transport have a significant impact on various business operations in the U.S., especially in middle America along hundreds of miles of the Mississippi River. However, inland water transportation is significantly affected by weather, current and future waterway conditions, and operation strategies at different locks, dams, and ports [11]. For example, in the case of flooding or drought, inland water transport will be constrained by the water levels of dams and ports, and the effects will propagate downstream. In response to such emergencies, goods on cargo vessels need to be offloaded and re-routed through the available ground transportation system. Since these infrastructures are managed by different governing agencies [3], multiple stakeholders need to understand the characteristics of these Interdependent Critical Infrastructures (ICIs), such as ports, lock and dam systems, and ground transportation that cross administrative boundaries. Considering the large potential impact and lack of actual data availability, this research will generate simulated data to represent a multimodal transportation systems.

1.2. Related work

There are various simulation models discussed in the literature that focus on inland waterway operations with different problems to solve and goals to achieve. However, the literature that studies the simulation of traffic flow in inland waterways can be broadly divided into three categories: (1) literature that focuses primarily on lock operation simulation models to analyze lock delays and travel times, and optimize waterway investment projects and other aspects of locks operations [12–14], (2) literature that discusses barge dispatching and vessel assignment scheduling problems in inland waterways [15–17], and (3) literature with a broader scope that considers ICI resilience, disruption management strategies and economic studies with a focus on inland waterways as the leading network of commodity flow [18–20].

There are multiple simulation models that were developed to analyze the different aspects of lock operations [12]; the earliest model can be found in 1969 [21] which was developed jointly by Resources for the Future Inc. and Pennsylvania State University. The model (referred to as RFF by [13]) was programmed to simulate the movement of shallow draft barge tows through a linear waterway having up to ten locks with one or two chambers, twenty ports, and ten delay points (channel restrictions). Model inputs include tow characteristics, tow itineraries, and attributes of the waterway system; model outputs include a variety of statistics including tows processed, transit and delay times, queue lengths, and tonnages [13,21]. Carroll and Bronzini [13] developed an enhanced two-part model of the RFF; the first part processes information concerning commodity flows and waterway fleet characteristics to derive a list of tows that will move on the Illinois waterway and upper Mississippi River, where the second part of the model simulates the movement of these tows through the ports, locks, pools, and channel delay areas that comprise the waterway system. Moreover, Dai [22] developed a waterway simulation model that estimates tow delays at a series of locks, tow travel time along waterways, and the means and variances of interarrival and interdeparture times at each lock; and was validated by comparing it to the well-established M/G/1 queue system. Additionally, Ting and Schonfeld [23] applied the simultaneous perturbation stochastic approximation (SPSA) technique with simulation models to optimize the size and timing of investment projects in a waterway system with five locks. The discussed lock operation simulation studies rely on site-specific simulation models without network generality and comprehensive functionality, making it difficult to extend the developed simulation models to any other waterway networks [12]. To address the lack of generalized modeling, Wang and Schonfeld [12] developed a general waterway simulation model that is independent of network geometry to evaluate a waterway system over a multi-year planning horizon. Recently, Triska et al. [14] developed a robust Monte Carlo simulation-based method to assess port capacity and expansion plans. Their method helps to identify optimal resource configurations for expected throughputs.

A second category of waterway simulation studies uses simulation as an optimization tool to solve the barge dispatching and assignment problem, which is generally solved using classical optimization approaches [17]. Larson et al. [15] developed a Barge Operations Systems Simulator (BOSS) to assist in the task of fleet sizing when transporting refuse from New York City to Fresh Kills Landfill on Staten Island. Moreover, Swedish [16] developed a discrete event simulation model as a decision support tool for logistical management within a marine-based distribution system to determine fleet size and resource allocation to meet delivery requirements in a timely manner. Taylor et al. [17] presented a simulation-based scheduling system designed to assist in barge dispatching and boat assignment problems for inland waterways.

Regarding the third category of literature, many studies have investigated the modeling and simulation of ICIs through empirical approaches, agent-based approaches, network-based approaches, and other approaches [20,24]. However, only few articles addressed simulation of inland waterways transportation [4]. Bush et al. [25] developed an iterative technique between optimization and simulation models to check the feasibility of barge routings suggested by the optimization model based on a sampled dataset. Biles et al. [26] presented a simulation model of traffic flow in inland waterways with the incorporation of the Geographic Information System (GIS) to improve vessel scheduling. Recently, Oztanriseven and Nachtmann [18] used a Monte

Carlo simulation model to estimate the potential economic impacts of inland waterway disruptions. Moreover, several studies investigated the economic impact of disruptions on different transportation systems [27–29]. Furthermore, Desquesnes et al. [19] created a simulation architecture of inland waterways based on Markov Decision Process (MDP) and climate projections under uncertainty. Bipasha et al. [4] developed an agent-based multimodal simulation tool, which is the initial study of the model presented in this article. With the exception of [4], all the studies in this third category do not consider predicting disruptions in advance based on statistical models, simulating multimodal transportation, modeling the interdependency between waterway transportation and ground transportation, and allowing different scenario generation by controlling lock and dam systems.

1.3. Overview and research contributions

The ultimate goal of this work is to provide research methods and application opportunities from which the U.S. economic growth and homeland security can significantly benefit. A thorough understanding of multimodal freight movement processes that combine different data sources can provide open-sourced, multi-regional, multi-industry, data-driven statistical models, and simulation tools to benefit decision-makers, researchers, and other stakeholders. Thus, various data elements from historical events of natural inland waterway disruptions such as floods and droughts along the Mississippi River and the McClellan–Kerr Arkansas River Navigation System (MKARNS) were used to develop a spatio-temporal statistical model [30,31]. This model predicts disruptions at different locations on both rivers, which guide the movement of multi-industry cargo vessels, operation of the lock-and-dam system in the area, and decisions regarding other modes of transportation for products shipped to and from inland waterway terminals.

The simulated data are derived from actual data on ICIs. The ICIs related data includes: (1) inland waterway and ground transportation networks (e.g., road type and capacity of road network) [32]; (2) locations of dams and locks [2,33,34]; (3) locations of major ports and their top commodities [2,3]; (4) historical hydrological observation data at ports and locks including water depth, changes in waterways, and the normal capacity of inland water transport [35]; (5) major types of cargo vessels and barges classified by their capacity and usual transport speed; and (6) weather data covering the studied regions [36]. Moreover, the Maritime Transportation Research and Education Center (MarTREC) at the University of Arkansas [37] provides the Transportation Resource Data Bank [38] that compiles rich information, such as freight commodity flow and ports. It is worth pointing out that, although the proposed simulation methods are centered on multimodal transportation networks, they can be used broadly in modeling other local, regional, and national infrastructures after proper modifications. Especially, the access to the most recent version of the open-sourced simulation tool addressed in this article is currently available for researchers, decision-makers, and other stakeholders to advance research on multimodal transportation systems [39].

The remainder of this article is organized as follows. Section 2 describes the development of the spatio-temporal statistical model used in this study and the basic features of the model. Section 3 introduces the simulation tool developed on an open-source platform. Section 4 presents a case study to illustrate the capabilities of the tool. Section 5 provides concluding remarks and future research directions.

2. Methodology

A hybrid methodology combining statistical analysis and simulation is applied. The statistical modeling is employed with two primary purposes: (1) to map the spatial fluctuations of gage height on a given river across sites, to interpolate spatially unobserved points on a river and (2) to forecast the gage height measurements on the sites of interest and anticipate possible interruptions in the flow of vessels. The simulation-based modeling is used to create scenarios for vessel and truck flow, utilizing the results from the statistical models. The dynamic interaction between different input parameters and simulation controls allows for the estimation of various metrics.

2.1. Geo-spatial model

Environmental variables are among the factors affecting the reliability of ICIs. To represent the waterway transportation network, modeling relevant variables of the corresponding water bodies, e.g., rivers, becomes central in understanding the processes that affect the availability of the infrastructures of interest. The selected statistical modeling approach must make accurate predictions and estimate the confidence intervals for relevant variables on the selected sites. To this end, developing a model capable of capturing the underlying relationship between the selected variables, the spatial correlation among the selected measuring sites and the associated variations in time is one of the key tasks in this stage. The chosen framework is *spTimer* [40], a spatio-temporal Bayesian modeling package using the R language for statistics. The main variable of interest is the Gage Height (GH), a measure of the water's depth filling the waterways on the measurement sites. The main purpose of this model is to generate data to estimate the GH on unobserved sites of interest. In this context, unobserved sites are selected locations with no available measurements, and it is necessary to infer the missing GH data from those from the observed sites. The model will learn a spatio-temporal mapping for the GH data from the observed sites and generate interpolations for new coordinates of interest along the same rivers.

The proposed model captures the seasonal variation for each site's time series of gage height measurements along with the spatial correlation in such measurements, driven by spatial location and their relation to each river. Although historical data over a long time interval is used to showcase the model's performance, the model is potentially useful for stakeholders to predict future conditions, even under changes in spatial or temporal structure. A potential approach, beneficial for planning and control, is to repeat the model fit as soon as more data is available and limit the prediction horizon to a short but useful time interval. For example, the model could be readjusted every week using a sliding window of two years of historical data with a one-week prediction horizon. This would guarantee that the model is up to date with the environmental conditions and that the predictions are current and informative.

Table 1
Summary of GH statistics.

Min	Q1	Median	Mean	Q3	Max
0.00	7.45	11.83	14.04	19.43	44.63

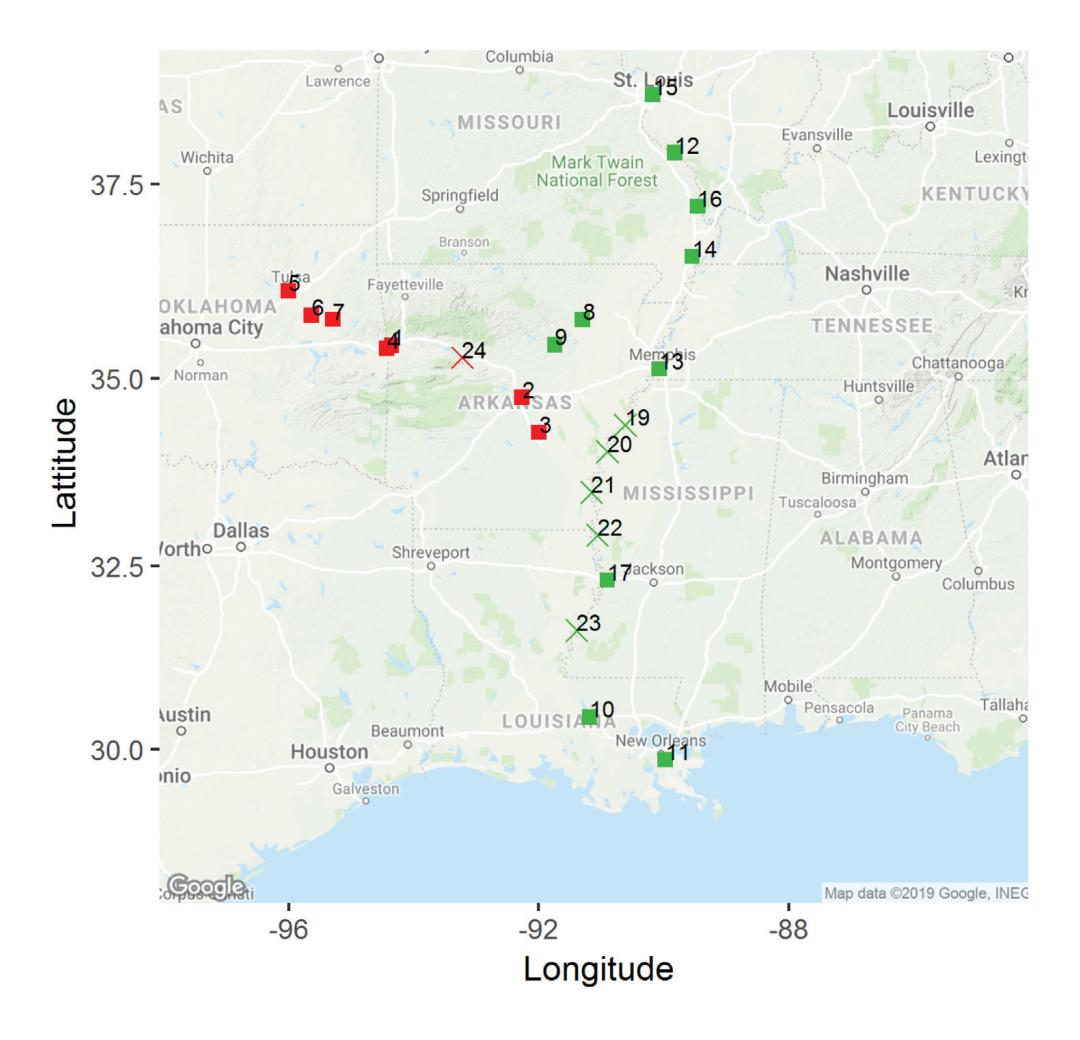


Fig. 1. Measurement sites by rivers.

2.2. Data

The data used corresponds to GH's hourly measurements and lock availability data in eighteen different sites, equivalent to eighteen geo-related time series, with 17,542 observations each (more than 315 million in total). From these, 22,961 are missing measurements, representing 7.3% of the total observations. A statistical summary of the GH measurements is shown in Table 1. The time window begins on February 22, 2016, and finishes on February 21, 2018. The observed sites are shown in Fig. 1. The sites are classified as connected to the MKARNS (red) or the Mississippi River (green). The selected unobserved locations of interest are marked with "X".

2.3. Theoretical background

To model the GH data, a hierarchical autoregressive model specifying distributions for data, process, and parameters in three stages is presented. The data is modeled by a Gaussian Process with spatio-temporal random effects. Model parameter estimation is conducted using Bayesian computation methods [40] implemented through Gibbs sampling with the *spTimer* package in R. A summary of the nomenclature is presented.

Nomenclature

i	Index for sites
l	Index for longer time unit (e.g., months)
t	Index for shorter time unit (e.g., hours)
r	Total number of longer units
T_l	Total number of shorter units
n	Number of sites
N	Total number of observations
s_i	The <i>i</i> th site
$Z_l(s_i, t)$	Observation at site i on time t
$O_l(s_i,t)$	True value of observation at site i and time t
$\epsilon_l(s_i, t)$	Error term at site i and time t
$\eta_l(s_i, t)$	Spatial random effect at site i and time t
\mathbf{Z}_{lt}	Vector of observations
\mathbf{O}_{lt}	Vector of true values
\mathbf{X}_{lt}	Matrix of covariates
ϵ_{lt}	Vector of error terms
$oldsymbol{\eta}_{lt}$	Vector of spatial random effects
Σ_{η}	Covariance matrix of spatial random effects
S_{η}	Spatial correlation matrix
$\kappa\left(\mathbf{s_i},\mathbf{s_j};\boldsymbol{\phi},\boldsymbol{\nu}\right)$	Correlation matrix entry for sites <i>i</i> and <i>j</i>
z	Matrix of observations
\mathbf{z}^*	Matrix of missing observations
θ	Vector of parameters
ρ	Temporal correlation parameter
β	Vector of covariate coefficients
$egin{array}{c} oldsymbol{eta} & \sigma^2_{\epsilon} \ \sigma^2_{\eta} & \phi \end{array}$	Pure error variance
σ_n^2	Spatial random effects variance
ϕ	Rate of decay of the spatial correlation
ν	Smoothness of the correlation function
μ_l	Mean of the autoregressive component on the /th time unit
σ_l^2	Variance of the autoregressive term on the <i>l</i> th time unit
ι	C

Let $Z_l(s_i,t)$ be the observed point-referenced data and $O_l(s_i,t)$ be the true value corresponding to $Z_l(s_i,t)$ at site s_i , $i=1,\ldots,n$ at time denoted by the two indices l and t, where l and t represent two units of time, for which l denotes the longer unit (e.g., months), $l=1,\ldots,r$, and t denotes the shorter unit (e.g., hours), $t=1,\ldots,T_l$. Note that r and T_l are the total numbers of the two time units, respectively. Define two vectors $\mathbf{Z}_{lt} = \left(Z_l\left(s_1,t\right),\ldots,Z_l\left(s_n,t\right)\right)^T$ and $\mathbf{O}_{lt} = \left(O_l(s_1,t),\ldots,O_l(s_n,t)\right)^T$. Let $N=n\sum_{l=1}^r T_l$ be the total number of observations to be modeled. The observed data is represented by \mathbf{z} and the missing data is denoted by \mathbf{z}^* . The hierarchical model used is expressed as follows with a description of variables and inputs, as presented in [40]:

$$\mathbf{Z}_{lt} = \mathbf{O}_{lt} + \boldsymbol{\epsilon}_{lt}$$

$$\mathbf{O}_{lt} = \boldsymbol{\rho} \mathbf{O}_{lt-1} + \mathbf{X}_{lt} \boldsymbol{\beta} + \boldsymbol{\eta}_{lt}$$
(1)

where $\epsilon_{lt} = (\epsilon_l(s_1,t),\dots,\epsilon_l(s_n,t))^T$ denotes the nugget effect (i.e., the pure error term) and is assumed to follow $N(\mathbf{0},\sigma_{\epsilon}\mathbf{I}_n)$, ρ is the temporal correlation parameter, and $\boldsymbol{\beta} = (\beta_1,\dots,\beta_p)$ represents the regression coefficients of the \mathbf{X} fixed effects or covariates. The spatio-temporal random effects are modeled by $\boldsymbol{\eta}_{lt} = (\eta_l(s_1,t),\dots,\eta_l(s_n,t))^T$, which is assumed to follow $N(\mathbf{0},\Sigma_\eta)$ and to be independent in time. Specially, $\Sigma_\eta = \sigma_\eta^2 S_\eta$, where σ_η^2 is the spatial variance assumed to be equal for all sites, and S_η is the spatial correlation matrix. In this article, S_η is obtained from the general Matérn correlation function [41], which is well suited to model a smooth process:

$$\kappa\left(\mathbf{s_{i}},\mathbf{s_{j}};\phi,\nu\right) = \frac{1}{2^{\nu-1}\Gamma(\nu)} (2\sqrt{\nu}\|s_{i} - s_{j}\|\phi)^{\nu} K_{\nu} (2\sqrt{\nu}\|s_{i} - s_{j}\|\phi), \phi > 0, \nu > 0$$
(2)

where $\Gamma(\nu)$ is the standard gamma function, K_{ν} is the modified Bessel function of second kind with order ν , $\|s_i - s_j\|$ is the distance between sites s_i and s_j , ϕ is the rate of decay of the spatial correlation, and ν is the smoothness parameter. Note that for the autoregressive component, ρ , it requires the specification of \mathbf{O}_{l0} , the initial term, for each l. For this purpose, an additional mean parameter μ_l and covariance matrix $\sigma_l^2 S_0$ must be estimated, with S_0 following the same structure as in Eq. (2).

Let $\theta = (\beta, \rho, \sigma_{\epsilon}^2, \sigma_{\eta}^2, \phi, \nu, \mu_l, \sigma_l^2)$ be the vector containing all the parameters of this model and $\pi(\theta)$ be the prior distribution of θ . The logarithm of the joint posterior distribution of the parameters and the observed and missing data for this model is given

by [40]:

$$\ln \pi \left(\boldsymbol{\theta}, \mathbf{O}, \mathbf{z}^* \mid \mathbf{z}\right) \propto -\frac{N}{2} \ln \sigma_{\epsilon}^2 - \frac{1}{2\sigma_{\epsilon}^2} \sum_{l=1}^{r} \sum_{t=1}^{T_l} \left(\mathbf{Z}_{lt} - \mathbf{O}_{lt}\right)^T \left(\mathbf{Z}_{lt} - \mathbf{O}_{lt}\right) - \frac{\sum_{l=1}^{r} T_l}{2} \ln \left|\sigma_{\eta}^2 S_{\eta}\right|$$

$$- \frac{1}{2\sigma_{\eta}^2} \sum_{l=1}^{r} \sum_{t=1}^{T_l} \left(\mathbf{O}_{lt} - \rho \mathbf{O}_{lt-1} - \mathbf{X}_{lt} \boldsymbol{\beta}\right)^T S_{\eta}^{-1} \left(\mathbf{O}_{lt} - \rho \mathbf{O}_{lt-1} - \mathbf{X}_{lt} \boldsymbol{\beta}\right)$$

$$- \frac{1}{2} \sum_{l=1}^{r} \ln \left|\sigma_{l}^2 S_{0}\right| - \frac{1}{2} \sum_{l=1}^{r} \frac{1}{\sigma_{l}^2} \left(\mathbf{O}_{l0} - \boldsymbol{\mu}_{l}\right)^T S_{0}^{-1} \left(\mathbf{O}_{l0} - \boldsymbol{\mu}_{l}\right)$$

$$+ \ln \left(\pi \left(\boldsymbol{\theta}\right)\right)$$
(3)

Using this posterior distribution and full conditionals as presented in [40], the estimation is carried out using Gibbs sampling. Then, the spatial interpolation or temporal extrapolation can be achieved using the predictive posterior for $Z_l(s_0, t')$ for any unobserved location s_0 and unobserved time point t':

$$\pi \left(Z_{l}(s_{0}, t') | \mathbf{z} \right) = \int \pi \left(Z_{l}(s_{0}, t') | O_{l}(s_{0}, t'), \sigma_{\varepsilon}^{2} \right) \times \pi \left(O_{l}(s_{0}, t') | \theta, \mathbf{O}, \mathbf{z}^{*} \right)$$

$$\times \pi \left(\theta, \mathbf{O}, \mathbf{z}^{*} | \mathbf{z} \right) dO_{l}(s_{0}, t') d\mathbf{O} d\theta d\mathbf{z}^{*}$$

$$(4)$$

3. Hybrid simulation model

This simulation model is developed using NetLogo, an agent-based programming language and simulation platform offered as freeware [42]. NetLogo is also a cross-platform and integrated environment for modeling both simple and complex systems that evolve dynamically. In NetLogo, "Agents" (turtle, link, patch, and observer) are the integral part of the NetLogo world and can follow instructions given by the designers. Turtles move around in the two-dimensional world, whereas the world contains a grid of patches. Every patch represents a square piece of land. All these agents can operate simultaneously without interfering with one another. NetLogo permits users to run the simulation in a browser or desktop application, interact with the software, and analyze its behavior under various settings [43].

3.1. Overview of the simulation model

The developed model was built on four extensions of NetLogo: GIS (Geographic Information System), R (R Language for Statistics), NW (Networks), and CSV (Comma Separated Values). GIS extension provides the ability to load vector GIS data in the form of ESRI shapefiles. The GIS extension is used to import several maps in the simulation model. Initially, a map of the U.S. is loaded as the base of NetLogo environment. Then, maps of inland waterways and highways are imported and drawn on top of the base map. Here, our simulation focus is primarily on the MKARNS and lower Mississippi River, representing the case study in this article (see Section 4). Fig. 2 shows NetLogo's user interface after opening and setting the basic environment of the model. The graphic window makes the two-dimensional "world" of the model visible. It is divided up into a grid of patches that have *pxcor* and *pycor* coordinates. The basic idea here is to create a NetLogo graph (nodes and links) by importing the GIS maps and creating vessel and truck "agents" that travel along with the links. The main components of the program are:

- A map of the United States, drawn on NetLogo in a simplified form. Each state border is drawn for reference. Figs. 3–4, provide
 a zoomed version of the interface.
- Maps of navigable waterways and highways. Both maps are made of nodes, turtles with own properties, connected by links.
 While the waterways/highways are only figurative, the nodes play an active role in the simulation because they facilitate the simulation understanding of waterways/highways maps.
- Vessels. These are turtles with their own variables such as current location, destination, distance-traveled, speed, vessel category (1 for large-sized, 2 for medium-sized, and 3 for small-sized), product weight, product type, extreme events, total delay, and others related to the control of the travel logic.
- Trucks. These are also turtles with properties such as current location, destination, distance-traveled, speed, product-weight, product-type, and others related to the control of the travel logic.
- Ports along the waterways. Eight ports are considered and modeled as a type of turtle. These are located in Tulsa, Fort Smith, Little Rock, Greenville (Mississippi), Baton Rouge, Helena, Memphis, and St. Louis along the MKARNS and Mississippi River. In Fig. 3, the yellow nodes represent the ports.
- · Fifteen locks along MKARNS. They are also made of nodes (a type of turtle) with properties such as ID and location.
- Twenty-four sites, modeled as turtles, along the MKARNS and Mississippi River. In each site, the gage height level is checked and a decision is made regarding whether the vessels will move forward or not. The red nodes in Fig. 3 represent the sites.
- An algorithm that makes the vessels and trucks move on the waterways and highways, respecting defined interaction rules of movement between source and destination, navigation time and speed, and other agents. For example, during the simulation, a vessel always takes the shortest path between its source and destination. The travel logic controls that a defined speed is enforced for each vessel and truck. The speed is defined when the vessel or truck is created as a random variate following a truncated exponential distribution. The range and mean of said distribution are parameters that can be controlled by the user.

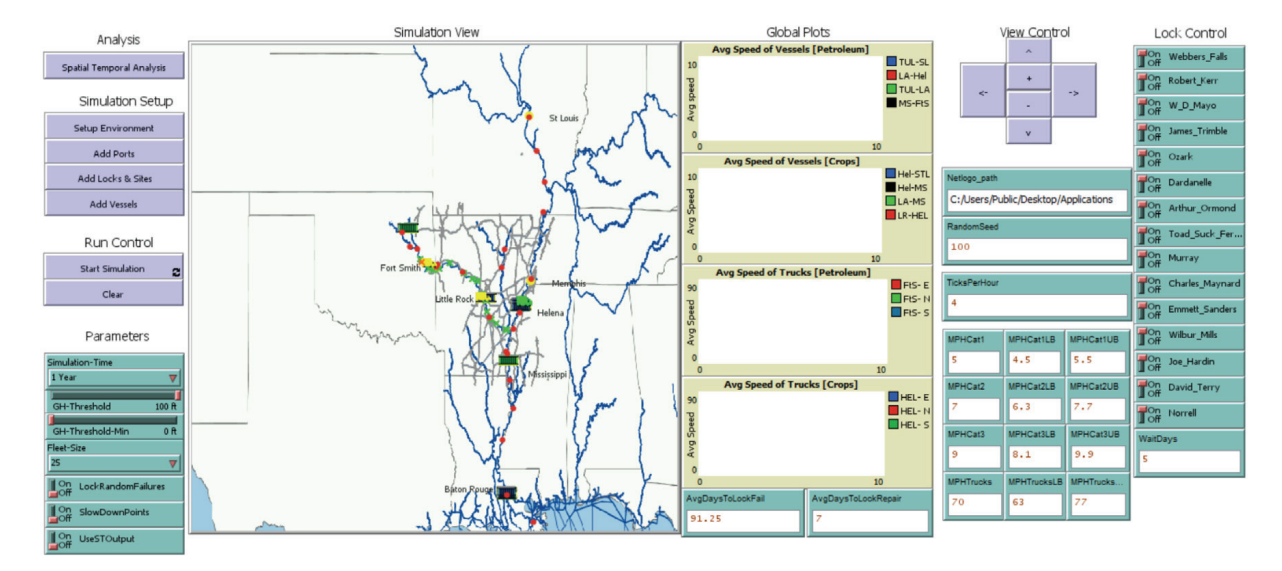


Fig. 2. Simulation model interface on NetLogo.

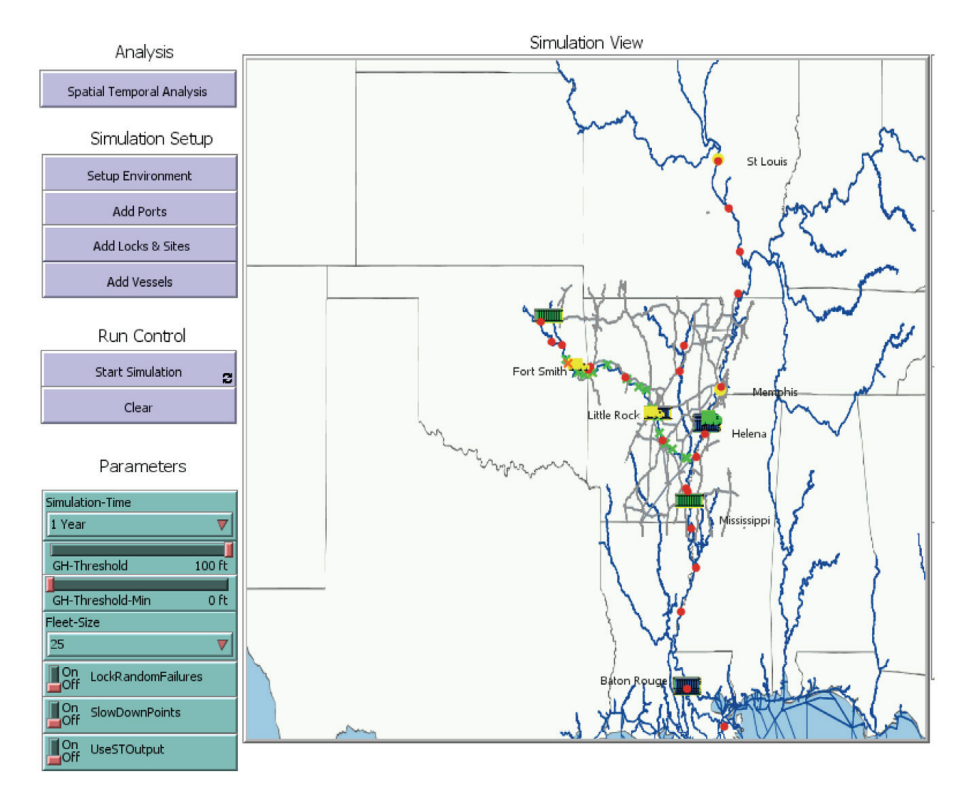


Fig. 3. Simulation model interface setup controllers in NetLogo.

During the simulation, each vessel and truck checks that the distance traveled along the next node in the path is consistent with its defined speed. If the distance is larger than what it should travel during a tick, it waits for another tick. If it is shorter than what it should travel, it progresses another step in the path and checks that the cumulative distance is consistent with the speed. If it encounters an obstacle in its path (e.g., a vessel facing an extreme event or disabled lock), it waits until the path is enabled again.

The main assumptions of our simulation model are as follows:

• Vessels are uniformly distributed based on the annual demand for commodities. The decisions for instantiating different vessels are encoded in the model following the times between departures designed to have a uniform distribution throughout the year.

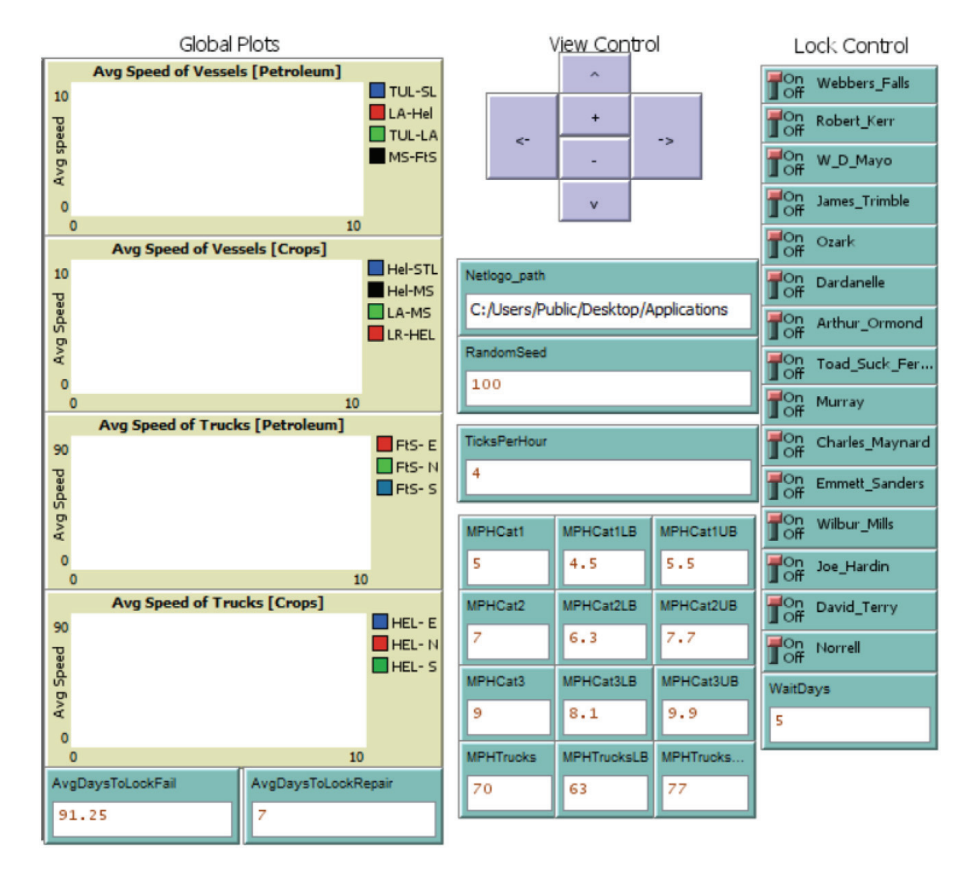


Fig. 4. Simulation model interface view and lock controllers in NetLogo.

- The speed of vessels varies with its capacity and size [26,44]. The smallest vessel is the fastest one with an average speed of nine mph. The medium-sized vessel moves at seven mph, where the largest one moves with five mph [26,44]. A truncated exponential distribution is used to draw random values for the speed each time a vessel is created in the simulation.
- · Each vessel and truck carries only one commodity type.
- · All the vessels and trucks travel only once to their predefined destinations and do not return to their origin ports.

3.2. Interdependencies of critical infrastructures

The functional interdependencies among ICIs are modeled by simulating a certain number of traveling cargo vessels along the waterways and a number of available ports with various capacities and conditions. In the case of a natural disturbance (e.g., elevated water levels), a decision of offloading and re-routing based on the expected size and duration of the disturbance and the current and future conditions of the ground transportation network is made. Given the flexibility of the proposed simulation model, different scenarios can be tested to assess the decision making process.

Additionally, another form of functional interdependency is available through the simulation of the interconnected operations of dam, lock, port, and ground transportation in case of traffic congestion or disruption. Considering such interdependencies of critical infrastructures and the multimodal transportation components, different scenarios involving human interactions, such as flood discharge, dredging, and use and maintenance of locks, can be analyzed. Furthermore, cost analysis approaches can be implemented to estimate the economic impact of commodity flow decisions.

Potential response plans will be simulated to help researchers understand how enacted emergency plans impact the multimodal transportation system and the surrounding infrastructure. Moreover, the developed agent-based simulation tool is capable of simulating the evacuation and re-routing processes, for which the system performance can be presented for different points in time. Thus, the interdependency among multiple decision-makers at ports, ground transportation, and government in this simulation environment can be captured to generate various scenarios. Such scenarios can help coordinate the efforts to optimize the decision making process for all stakeholders involved.

4. Case study

4.1. Problem description

In the simulation, the system analyzes a pre-determined set of representative quantities based on the input parameters listed in Table 2. In addition, Fig. 5 represents a sample run and Fig. 6 shows a sample of plots that were generated during the simulation.

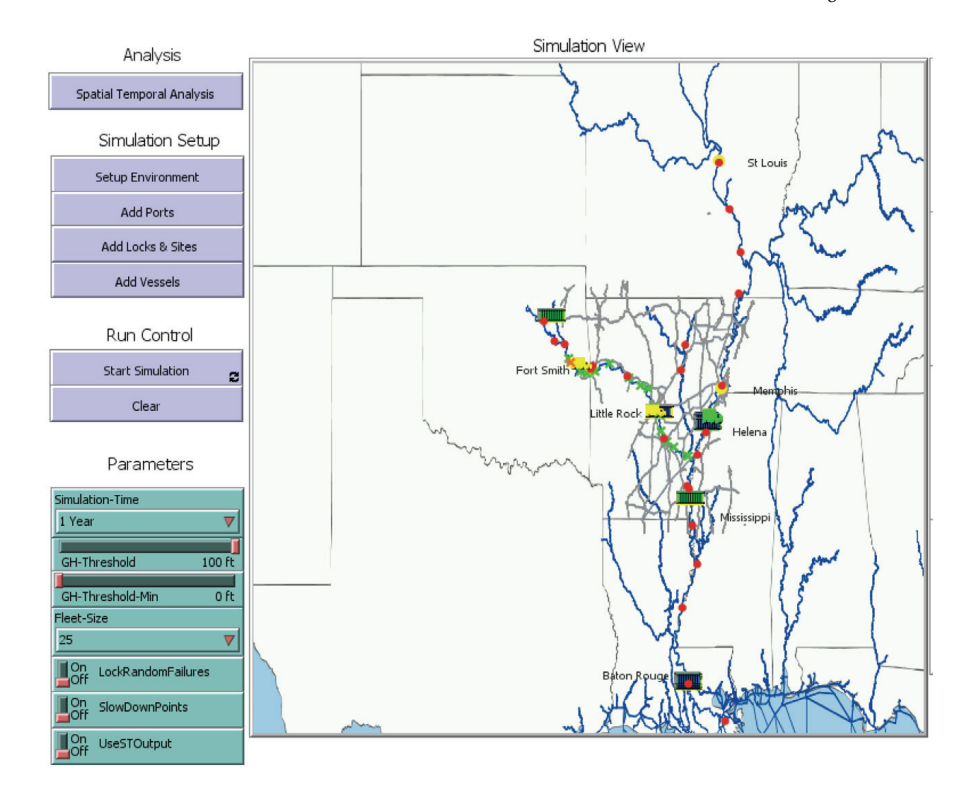


Fig. 5. Simulation running on NetLogo.

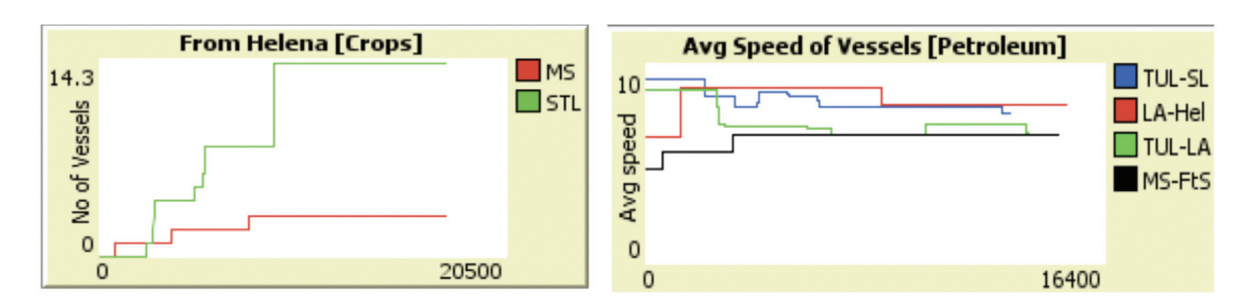


Fig. 6. Instantaneous plotting information while simulation is running on NetLogo.

 $\begin{tabular}{ll} \textbf{Table 2} \\ \begin{tabular}{ll} \textbf{The main inputs and outputs of the developed simulation tool.} \\ \end{tabular}$

Model Inputs	Model Outputs
Gage height from a spatio-temporal model	Average speed of each vessel category between every two ports (mph)
 Supply and demand between ports (movement of commodities) 	Number of delays between every two ports
Gage height threshold limit	Total time lost due to extreme events (hour)
Lock availability	Total number of vessels delayed and their tonnages
Vessel distribution at each port	 Overall average speeds for the three types of vessels (mph)
Fleet size	• Number of extreme events and length (time) in MKARNS and lower Mississippi River
Number of trucks	· Number of vessels from each category traveled and arrived between every two ports
	 Average speed of trucks for each product type (mph)

Table 3
Detail on simulation scenarios.

Scenario	Lock failures	GH measurements	Unobserved sites		
Base Case	Real observations	Real observations	Not included		
Random Lock Failures	Randomly generated	Real observations	Not included		
Spatio-temporal model	Real observations	Predictions from model	Interpolated from model		

Table 4
Summary of vessels' statistics for the base-case simulation runs

From	То	Product type	Vessel category	Vessel count	Weight (ktons)	Average Speed (mph)	Extreme events	Distance (miles)	Total delay (hours)
Baton Rouge	Helena	Petroleum	1	1	18	3.79	0	540.69	0
Baton Rouge	Helena	Petroleum	2	1	12	7.83	0	540.30	0
Baton Rouge	Helena	Petroleum	3	1	6	10.65	0	548.47	0
Baton Rouge	Mississippi	Crops	1	3	54	4.20	1	355.04	1
Baton Rouge	Mississippi	Crops	2	4	48	9.06	0	376.49	0
Baton Rouge	Mississippi	Crops	3	8	48	10.88	3	360.63	2.5
Baton Rouge	Mississippi	Petroleum	1	1	18	3.53	1	356.43	1
Baton Rouge	Mississippi	Petroleum	2	1	12	8.74	0	342.95	0
Baton Rouge	Mississippi	Petroleum	3	1	6	10.90	0	375.89	0
Helena	Baton Rouge	Petroleum	1	1	18	4.41	0	549.37	0
Helena	Baton Rouge	Petroleum	2	1	12	8.04	0	552.42	0
Helena	Baton Rouge	Petroleum	3	1	6	10.76	0	546.18	0
Helena	Mississippi	Crops	1	1	18	3.79	0	186.45	0
Helena	Mississippi	Crops	2	1	12	6.35	0	182.55	0
Helena	Mississippi	Crops	3	1	6	10.11	0	164.31	0
Helena	Mississippi	Petroleum	1	1	18	3.90	0	170.69	0
Helena	Mississippi	Petroleum	2	1	12	6.94	0	173.61	0
Helena	Mississippi	Petroleum	3	1	6	10.42	0	198.04	0
 Helena	St. Louis	Crops	1	3	54	3.69	0	603.78	0
Helena	St. Louis	Crops	2	4	48	8.72	0	604.63	0
Ielena	St. Louis	Crops	3	7	42	10.44	0	600.64	0
ittle Rock	Helena	Crops	1	12	216	4.40	0	222.02	0
ittle Rock	Helena	Crops	2	18	216	7.67	0	221.72	0
ittle Rock	Helena	Crops	3	31	186	10.25	0	222.14	0
Aississippi	Baton Rouge	Crops	1	6	108	3.75	2	381.82	1.5
Mississippi	Baton Rouge	Crops	2	8	96	9.06	3	380.19	3
Mississippi	Baton Rouge	Crops	3	16	96	11.03	1	382.06	1
Aississippi	Baton Rouge	Petroleum	1	1	18	4.07	1	379.89	1
Aississippi Aississippi	Baton Rouge	Petroleum	2	1	12	8.43	0	381.25	0
Aississippi Aississippi	Baton Rouge	Petroleum	3	1	6	10.38	1	378.96	0.5
Aississippi Aississippi	Fort Smith	Petroleum	1	1	18	4.33	0	445.88	0.5
Aississippi Aississippi	Fort Smith	Petroleum	2	1	12	7.65	0	441.58	0
Iississippi Iississippi	Fort Smith	Petroleum	3	1	6	11.42	0	445.21	0
Aississippi Aississippi	St. Louis	Crops	1	10	180	4.01	0	766.42	0
Aississippi Aississippi	St. Louis	Crops	2	15	180	8.12	0	766.67	0
Aississippi Aississippi	St. Louis	Crops	3	29	174	10.29	0	765.51	0
ilsa:	Baton Rouge	Petroleum	1	5	90	4.64	4	992.74	4
'ulsa	Baton Rouge	Petroleum	2	5 7	90 84	8.13	2	989.29	2
'ulsa	Baton Rouge	Petroleum	3	13	78	10.87	6	989.29	6
'ulsa	Helena	Petroleum	1	1	18	4.26	0	621.25	0
ulsa 'ulsa	Helena	Petroleum	2	1	12	8.01	0	612.57	0
ulsa	Helena	Petroleum	3	2	12	10.26	0	620.40	0
			1	2	36		0		0
'ulsa 'ulsa	Memphis	Petroleum Petroleum	2	3	36 36	4.42 8.02	0	691.78 693.74	0
	Memphis		3				0		0
'ulsa	Memphis	Petroleum		6 3	36	10.32	0	693.14	
'ulsa	Mississippi	Petroleum	1 2	3 5	54	4.73		613.82	0
'ulsa	Mississippi	Petroleum		5 9	60 54	8.30	0	624.32	0
'ulsa	Mississippi	Petroleum	3	-		10.70		625.59	
Culsa	St. Louis	Petroleum	1	4	72	4.08	3	1222.94	107.5
ľulsa	St. Louis	Petroleum	2	6	72	7.44	1	1217.46	190.5
Tulsa	St. Louis	Petroleum	3	12	72	8.54	4	1217.97	820.25

We generate an output file at the end of the simulation which presents all the measurements listed above. The simulation time is set for 12 months (1 year), the fleet size is set to 25 trucks, and GH global threshold is 100 ft with individual thresholds set to action stage level based on the National Weather Service (NWS) data [45]. Initially, vessels began from the ports of Tulsa, Baton Rouge, Little Rock, Greenville, and Helena, and the locks were all open. The vessels were moving towards their destination ports, and extreme events were checked by measuring gage height and lock availability at each site. For example, the vessels passing the sites with GH greater than the allowable threshold between the LA-MS route along the Mississippi River could not move and had to wait until the GH level falls below the threshold. Whenever a vessel faces any extreme event and stops moving forward, its color turns red to represent a stoppage. The vessel gets back to its original color when movement resumes. If the disruption is prolonged, it may potentially inhibit the vessel from reaching its destination. This is moderated by the parameter "WaitDays" that controls the number of days a given barge waits before detouring into ground transportation as an alternative. To illustrate the capability of the model, three different simulation runs covering few different aspects of available inputs were generated. First, a base-case run is generated without including the developed spatio-temporal statistical model with level predictions or possibility of random lock

Table 5
Summary of vessels' statistics for the random lock failure case

rom	То	Product type	Vessel category	Vessel count	Weight (ktons)	Average Speed (mph)	Extreme events	Distance (miles)	Total delay (hours
Baton Rouge	Helena	Petroleum	1	1	18	3.79	0	536.62	0
Baton Rouge	Helena	Petroleum	2	1	12	7.79	0	541.13	0
Baton Rouge	Helena	Petroleum	3	1	6	10.66	0	559.80	0
Baton Rouge	Mississippi	Crops	1	3	54	4.16	2	361.48	2
Baton Rouge	Mississippi	Crops	2	4	48	8.79	3	364.60	2.75
Baton Rouge	Mississippi	Crops	3	8	48	10.85	2	354.17	2
Baton Rouge	Mississippi	Petroleum	1	1	18	3.49	1	372.51	1
Baton Rouge	Mississippi	Petroleum	2	1	12	8.79	0	362.73	0
Baton Rouge	Mississippi	Petroleum	3	1	6	10.86	0	361.19	0
Helena	Baton Rouge	Petroleum	1	1	18	4.41	0	537.93	0
Helena	Baton Rouge	Petroleum	2	1	12	8.00	0	539.78	0
Helena	Baton Rouge	Petroleum	3	1	6	10.75	0	548.47	0
Helena	Mississippi	Crops	1	1	18	3.74	0	187.75	0
Helena	Mississippi	Crops	2	1	12	6.20	0	175.08	0
Helena	Mississippi	Crops	3	1	6	10.34	0	191.32	0
Helena	Mississippi	Petroleum	1	1	18	3.90	0	164.87	0
Helena	Mississippi	Petroleum	2	1	12	7.07	0	178.47	0
Helena	Mississippi	Petroleum	3	1	6	10.34	0	180.94	0
Helena	St. Louis	Crops	1	3	54	3.68	0	606.06	0
Ielena	St. Louis	Crops	2	4	48	8.73	0	601.40	0
Ielena	St. Louis	Crops	3	7	42	10.45	0	601.31	0
ittle Rock	Helena	Crops	1	12	216	4.38	0	224.75	0
ittle Rock	Helena	Crops	2	18	216	7.63	0	226.20	0
ittle Rock	Helena	Crops	3	31	186	10.33	0	224.12	0
/lississippi	Baton Rouge	Crops	1	6	108	4.11	3	382.48	3
Mississippi	Baton Rouge	Crops	2	8	96	8.49	3	381.50	3
Mississippi	Baton Rouge	Crops	3	16	96	10.92	5	382.18	4
Aississippi	Baton Rouge	Petroleum	1	1	18	4.12	0	381.25	0
/lississippi	Baton Rouge	Petroleum	2	1	12	8.43	0	379.39	0
/lississippi	Baton Rouge	Petroleum	3	1	6	10.48	0	379.89	0
Mississippi	Fort Smith	Petroleum	1	1	18	4.32	0	442.14	0
Mississippi	Fort Smith	Petroleum	2	1	12	7.64	0	445.21	0
Aississippi	Fort Smith	Petroleum	3	1	6	11.38	0	440.96	0
Aississippi	St. Louis	Crops	1	10	180	4.00	0	767.11	0
Aississippi	St. Louis	Crops	2	15	180	8.23	0	766.19	0
Aississippi Aississippi	St. Louis	Crops	3	29	174	10.23	0	768.11	0
'ulsa	Baton Rouge	Petroleum	1	5	90	4.45	2	992.51	2
'ulsa	Baton Rouge	Petroleum	2	7	84	8.35	3	994.31	1.75
'ulsa	Baton Rouge	Petroleum	3	13	78	10.93	3	990.76	2.5
'ulsa	Helena	Petroleum	1	1	18	4.77	0	612.57	0
'ulsa	Helena	Petroleum	2	1	12	8.14	0	614.94	0
'ulsa	Helena	Petroleum	3	2	12	10.81	0	617.21	0
'ulsa	Memphis	Petroleum	1	2	36	4.64	0	692.79	0
ulsa 'ulsa	Memphis	Petroleum	2	3	36	7.11	0	692.13	0
ulsa 'ulsa	Memphis	Petroleum	3	6	36	10.45	1	692.36	1
'ulsa	Mississippi	Petroleum	1	3	54	4.71	0	631.48	0
'ulsa	Mississippi	Petroleum	2	5 5	60	7.87	1	631.82	1
ulsa Tulsa		Petroleum	3	9	54	7.87 11.13	0	634.82	0
uisa 'ulsa	Mississippi St. Louis	Petroleum	3 1	4	5 4 72	4.02	0		0
uisa Tulsa	St. Louis St. Louis		2		72 72		3	1217.46 1222.25	
	at. Louis	Petroleum	4	6	14	7.71	S	1444.45	231.75

failures. Second, a run that includes random lock failures was generated to show how the model handles new input data and how output results are affected. Third, the spatio-temporal statistical model is used to predict water levels; hence, it predicts extreme events resulting from elevated water levels. To validate the spatio-temporal statistical model predictions, we provide water level time series comparisons with our available true data for multiple sites. A summary of these conditions is presented in Table 3.

For the scope of the current model, random lock failures are assumed to follow exponential distributions, both for the time between failures and time between repairs. Locks are initiated in a working state, and the time until the next failure is drawn from the exponential distribution with the mean time of three months as the default value. The time to complete a repair is drawn from the exponential distribution with the mean time of one week as the default value. The alternation of states is continued until the simulation run ends. Note that the mean time to failure and the mean time to repair have been coded as two parameters that the user can modify as needed.

Moreover, when a vessel reaches its destination port, trucks are used to carry its products to the final destinations. Fig. 6 (left) shows the number of vessels that were used to carry products (Crops) between two ports. At the end of the simulation, we generate

Table 6
Summary of vessels' statistics for the spatio-temporal model

rom	То	Product type	Vessel category	Vessel count	Weight (ktons)	Average Speed (mph)	Extreme events	Distance (miles)	Total delay (hours
Baton Rouge	Helena	Petroleum	1	1	18	3.79	0	540.69	0
Baton Rouge	Helena	Petroleum	2	1	12	7.81	0	541.12	0
Baton Rouge	Helena	Petroleum	3	1	6	10.66	0	541.13	0
Baton Rouge	Mississippi	Crops	1	3	54	4.19	0	372.45	0
Baton Rouge	Mississippi	Crops	2	4	48	9.05	0	368.37	0
Baton Rouge	Mississippi	Crops	3	8	48	10.94	0	359.85	0
Baton Rouge	Mississippi	Petroleum	1	1	18	3.53	0	382.63	0
Baton Rouge	Mississippi	Petroleum	2	1	12	8.73	0	340.31	0
Baton Rouge	Mississippi	Petroleum	3	1	6	10.89	0	362.05	0
Helena	Baton Rouge	Petroleum	1	1	18	4.41	0	549.37	0
Helena	Baton Rouge	Petroleum	2	1	12	8.02	0	555.68	0
Helena	Baton Rouge	Petroleum	3	1	6	10.67	0	557.39	0
Helena	Mississippi	Crops	1	1	18	3.79	0	186.45	0
Helena	Mississippi	Crops	2	1	12	6.32	0	172.26	0
Helena	Mississippi	Crops	3	1	6	10.11	0	161.73	0
Helena	Mississippi	Petroleum	1	1	18	3.93	0	167.99	0
Helena	Mississippi	Petroleum	2	1	12	6.73	0	159.89	0
Helena	Mississippi	Petroleum	3	1	6	10.43	0	185.07	0
Helena	St. Louis	Crops	1	3	54	3.68	0	605.75	0
Helena	St. Louis	Crops	2	4	48	8.72	0	608.37	0
Helena	St. Louis	Crops	3	7	42	10.45	0	606.94	0
ittle Rock	Helena	Crops	1	12	216	4.40	0	224.23	0
ittle Rock	Helena	Crops	2	18	216	7.67	0	221.62	0
Little Rock	Helena	Crops	3	31	186	10.26	0	221.21	0
Mississippi	Baton Rouge	Crops	1	6	108	3.76	0	382.54	0
Mississippi	Baton Rouge	Crops	2	8	96	9.12	0	384.15	0
Mississippi	Baton Rouge	Crops	3	16	96	11.05	0	382.47	0
Mississippi	Baton Rouge	Petroleum	1	1	18	4.12	0	390.17	0
Mississippi	Baton Rouge	Petroleum	2	1	12	8.40	0	377.97	0
Mississippi	Baton Rouge	Petroleum	3	1	6	10.40	0	390.17	0
Mississippi	Fort Smith	Petroleum	1	1	18	4.33	0	445.88	0
Mississippi	Fort Smith	Petroleum	2	1	12	7.65	0	441.58	0
Mississippi	Fort Smith	Petroleum	3	1	6	11.41	0	442.14	0
Mississippi	St. Louis	Crops	1	10	180	4.01	0	766.41	0
Mississippi	St. Louis	Crops	2	15	180	8.12	0	767.70	0
Mississippi	St. Louis	Crops	3	29	174	10.29	0	765.47	0
Tulsa	Baton Rouge	Petroleum	1	5	90	4.65	0	995.40	0
Tulsa Tulsa	Baton Rouge	Petroleum	2	7	84	8.14	0	992.99	0
Tulsa Tulsa	Baton Rouge	Petroleum	3	13	78	10.92	0	993.82	0
ruisa Tulsa	Helena	Petroleum	1	1	18	4.26	0	612.57	0
ruisa Tulsa	Helena	Petroleum	2	1	12	8.01	0	612.57	0
Tulsa	Helena	Petroleum	3	2	12	10.25	0	619.71	0
Tulsa	Memphis	Petroleum	1	2	36	4.43	0	692.60	0
'ulsa	Memphis	Petroleum	2	3	36	8.02	0	692.70	0
Tulsa	Memphis	Petroleum	3	6	36	10.31	0	690.98	0
Tulsa Tulsa	Mississippi	Petroleum	1	3	54	4.71	0	619.98	0
ruisa Tulsa	Mississippi	Petroleum	2	5 5	60	8.31	0	634.12	0
ruisa Fulsa	Mississippi	Petroleum	3	9	54	10.70	0	630.51	0
ruisa Tulsa		Petroleum	3 1	4	72	4.09	1	1222.59	106.5
ı uısa Fulsa	St. Louis St. Louis	Petroleum	2	6	72 72	4.09 7.44	1		106.5
เนเรส	St. LOUIS	renoieum	∠	O	14	7.44	1	1219.24	191.5

an output report summarizing multiple statistics of vessel (e.g., average speed and the number of extreme events) and truck behavior and summary plots (e.g., boxplots) that help the user understand varying aspects of the hybrid model.

4.2. Simulation results

This subsection reports the results obtained for a one-year base-case simulation run for the lower Mississippi River and MKARNS and compares selected results with the other two runs. These results are shown in Tables 4–7 and Figs. 7–9. Table 4 shows summary statistics for vessels traveled between every two ports classified by the vessel category, where category 1 represents small-sized vessels carrying up to 6 ktons of cargo, category 2 represents medium-sized vessels carrying up to 12 ktons of cargo, and category 3 represent large-sized vessels carrying up to 18 ktons of cargo. Table 4 information includes the number of vessels that have traveled between every pair of ports, average speed of travel, product type carried (petroleum or crops in our case), records of vessel category, and the total weight of carried products (in kilo tons). The number of extreme events (disruptions) faced by the

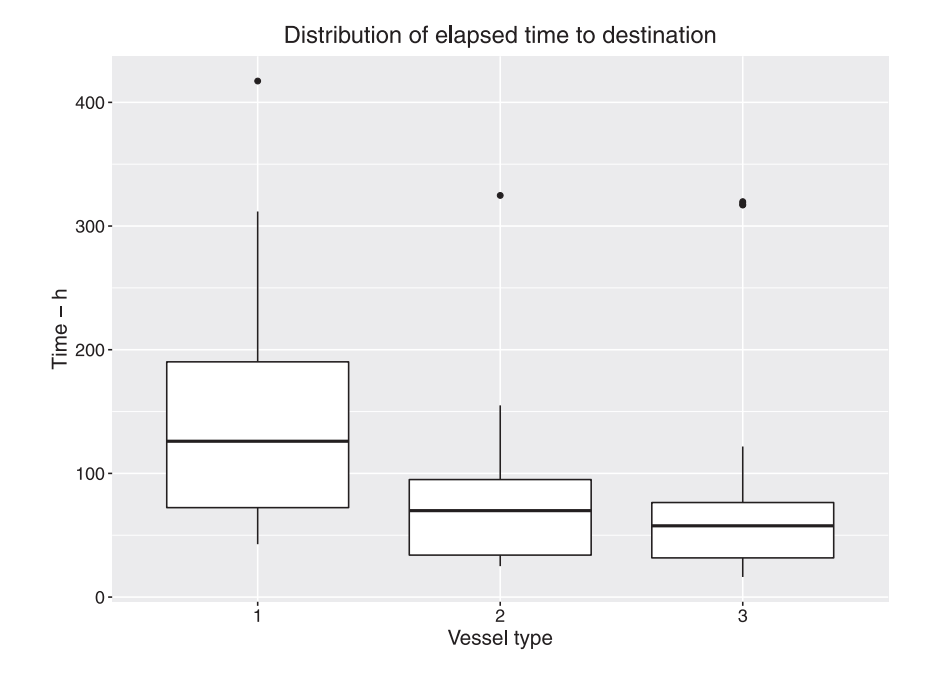


Fig. 7. Simulation model output of time to reach destinations for vessels in different categories (in hours).

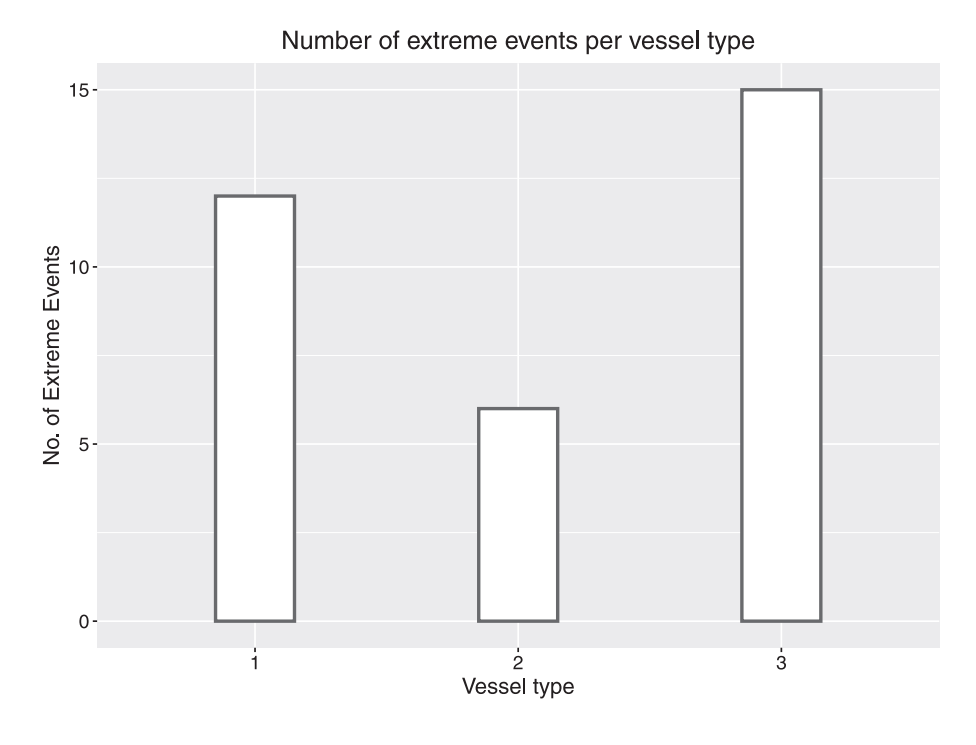


Fig. 8. Number of extreme events for vessels in different categories.

vessels is shown, where a disruption occurs in our setting whenever the water level exceeds a predefined threshold. The total delay (in hours) caused by such disruptions and the distance traveled by vessels are also recorded. Some of these statistical summaries are plotted such as the ones in Figs. 7–9 showing a boxplot of the distributed time to destination, a bar chart of number of extreme events by vessel category, and a boxplot of average speed of each vessel category, respectively. The outputs of the simulation model also include detailed information about all vessels appeared in the model (see Table 8 in Appendix). Like the records mentioned before, the detailed information includes the product type carried, category of the vessel, total weight of the product, and a defined ID for each vessel (modeled as a turtle). Also registered, each vessel's start time, time of departure from its origin, and its end time

Distribution of average speed per vessel type (3 is the fastest) 7.5 5.0 Vessel type

Fig. 9. Average speeds of vessels in different categories (mph).

(time of arrival at its destination). These records can help extend the simulation analysis and contribute to the model's debugging and validation. Table 7 shows summary statistics for trucks traveled from all ports to four defined exit points labeled as cardinal directions (i.e., East, West, North, and South) located at the edges of the studied area. For example, we have 16 fleets of trucks that have traveled from the Fort Smith port to the eastern exit point with an average speed of 71.57 mph. Trucks that reach these boundary points are assumed to have left the area to other states to deliver goods. There are four random chosen boundary points located at the east, west, south and north of the studied area map. To model possible delays (disruptions) of trucking-delivery of goods, possible congestion on the highways is represented using "slow down points" which are sections where truck speed is reduced, generating a similar behavior of possible congestion on the road. This feature of the simulation model is useful when considering commodity flow planning with information about traffic data. These results are available with additional detailed information about the trucks, as shown in Table 9 in Appendix.

Comparing the results for the base-case scenario with the random lock failures (shown in Table 5), one can observe an overall increase in the total delay hours for random lock failures. In fact, the total delay in hours for the base-case scenario is about 1,141 h compared to approximately 1,474 hours for the case of random lock failure. This shows that the model responds as expected to changes across simulation runs. For the third case (i.e.,spatio-temporal predictions) shown in Table 6, one can see that there is no significant difference between the model's final output of approximately 1,122 h of delay compared to the base-case one with 1,141 h. This shows that the developed spatio-temporal statistical model is predicting close water levels compared to the actual data available used in the base-case run. In addition, to validate the spatio-temporal model predictions of water levels, Fig. 10 compares the predicted values (with a 90% point-wise confidence band) to the real observed data in two selected sites. Two important elements can be seen in Fig. 10: (1) the prediction captures the seasonality of the actual data and (2) the trend of the spatio-temporal statistical model behaves as the actual data. Specially, the developed statistical model captures both trend and seasonality with a low mean squared error (MSE) of 1.7 ft² for the fitted values vs. the GH observations.

5. Conclusions and future research

In this study, multiple contributions are made to the ICIs risk analysis and commodity flow literature. First, a spatio-temporal statistical model was developed to capture extreme natural events causing disruptions in inland waterways and predict them in the future to facilitate commodity flow planning and response actions. The developed statistical model can also handle missing data without a noticeable degradation in its overall performance. In addition, the statistical model was developed and tested on the lower Mississippi River and the MKARNS. Second, a simulation tool is built to capture the effect of inland waterways disruptions on the commodity flow through other ICIs, which provides a broad understanding of the multimodal transportation system interdependencies in action. Third, access to the most recent version of the simulation model is currently available as an open-sourced tool for researchers, decision-makers, and other stakeholders to advance research in multimodal transportation [39].

0

2016-07

2016-07

40-30-20-10-

Gauge Height for site 8

— GH — Model Fit

Date and Time Gauge Height for site 10 — GH — Model Fit

2017-07

2017-07

2018-01

2018-01

2017-01

40-40-30-10-10-

Fig. 10. Water levels (in ft) predicted by the Spatio-temporal statistical model vs. actual data at some selected sites.

Date and Time

2017-01

The current version of the model has limitations that can be reduced by this research team or potential users of this open-sourced tool. Especially, distributing vessels uniformly over time might not be the best representation of real demand as it most likely is not stationary and presents some forms of seasonality. This is a promising research direction that can be explored in the future. Another limitation is the capability of the statistical model for emulating outliers in predicting GH measurements. The current model uses a Bayesian Gibbs sampling approach that relies on the mean of sampled predictions. This may lead to conservative estimates. Clearly, emphasis on this limitation can be another valuable research direction.

This work could be extended to support emergency service response and detailed analysis of ports operations. In addition, national economic and transportation studies centered on inland waterways and their interdependency with ground transportation can be investigated by extending the developed simulation tool to include features such as private trucking companies routes, real-time traffic data, and railroads information. An economic study based on the developed simulation tool covering the current case study is among the near future research directions.

Table 7
Summary of trucks' statistics for the base-case simulation runs.

From	Product type	Destination	Count	Avg. speed (mph)
Fort Smith	Petroleum	Е	16	71.57
Fort Smith	Petroleum	N	2	68.99
Fort Smith	Petroleum	S	2	67.42
Helena	Crops	E	61	68.32
Helena	Crops	N	61	68.78
Helena	Crops	S	61	61.41
Helena	Petroleum	E	16	66.25
Helena	Petroleum	N	2	69.35
Helena	Petroleum	S	2	57.92

Table 8
Detailed outputs for vessels.

Product type	ID	Distance traveled	Weight (ktons)	Vessel category	Extreme events	Total delay (hours)	Avg. speed (mph)	End time (ticks)	Start time (ticks)	From	То	Time elapse (ticks)
Petroleum	3	548.47	6	3	0	0	10.65	1551.75	1500.25	Baton Rouge	Helena	51.5
Petroleum	4	356.43	18	1	1	1	3.53	601.25	500.25	Baton Rouge	Mississippi	101
Petroleum	5	342.95	12	2	0	0	8.74	2539.5	2500.25	Baton Rouge	Mississippi	39.25
Petroleum	6	375.89	6	3	0	0	10.90	4534.75	4500.25	Baton Rouge	Mississippi	34.5
Petroleum	100	549.37	18	1	0	0	4.41	124.5	0	Helena	Baton Rouge	124.5
Petroleum	101	552.42	12	2	0	0	8.04	4569	4500.25	Helena	Baton Rouge	68.75
Petroleum	102	546.18	6	3	0	0	10.76	6301	6250.25	Helena	Baton Rouge	50.75
Petroleum	103	170.69	18	1	0	0	3.90	1294	1250.25	Helena	Mississippi	43.75
Petroleum	104	173.61	12	2	0	0	6.94	5525.25	5500.25	Helena	Mississippi	25
Petroleum	105	198.04	6	3	0	0	10.42	2519.25	2500.25	Helena	Mississippi	19
Petroleum	200	445.88	18	1	0	0	4.33	103	0	Mississippi	Fort Smith	103
Petroleum	201	441.58	12	2	0	0	7.65	1558	1500.25	Mississippi	Fort Smith	57.75
Petroleum	202	445.21	6	3	0	0	11.42	4289.25	4250.25	Mississippi	Fort Smith	39
Petroleum	203	379.89	18	1	1	1	4.07	593.5	500.25	Mississippi	Baton Rouge	93.25
Petroleum	204	381.25	12	2	0	0	8.43	2545.5	2500.25	Mississippi	Baton Rouge	45.25
Petroleum	205	378.96	6	3	1	0.5	10.38	5036.75	5000.25	Mississippi	Baton Rouge	36.5
Petroleum	346	693.08	18	1	0	0	4.38	161	2.75	Tulsa	Memphis	158.25
Petroleum	359	1226.83	18	1	1	1	4.49	275.75	2.75	Tulsa	St. Louis	273
Petroleum	371	1219.62	6	3	0	0	10.58	118	2.75	Tulsa	St. Louis	115.25
Petroleum	378	1221.13	6	3	0	0	10.85	115.25	2.75	Tulsa	St. Louis	112.5
Petroleum	322	989.20	6	3	0	0	10.87	93.75	2.75	Tulsa	Baton Rouge	91
Petroleum	369	1215.23	6	3	1	206.5	3.83	817.5	500.25	Tulsa	St. Louis	317.25
Petroleum	376	1218.30	6	3	1	202.5	3.81	820	500.25	Tulsa	St. Louis	319.75
Petroleum	357	1216.69	18	1	1	105.5	2.92	917.5	500.25	Tulsa	St. Louis	417.25
Petroleum	310	987.27	12	2	0	0	8.81	612.25	500.25	Tulsa	Baton Rouge	112
	372	1219.62	6	3	1	208	3.85	817.25	500.25	Tulsa		317
Petroleum Petroleum	374	1219.62	6	3	1	203.25	3.82	819	500.25	Tulsa	St. Louis St. Louis	318.75
					0							
Petroleum	330	610.70	18 12	1 2		0 190.5	4.41	638.75	500.25	Tulsa	Mississippi	138.5
Petroleum	363	1213.83			1		3.74	825	500.25	Tulsa	St. Louis	324.75
Crops	1014	591.24	6	3	0	0	11.00	5304	5250.25	Helena	St. Louis	53.75
Crops	1015	600.07	6	3	0	0	9.88	5311	5250.25	Helena	St. Louis	60.75
Crops	1016	607.05	6	3	0	0	9.99	5311	5250.25	Helena	St. Louis	60.75
Crops	1200	355.85	18	1	0	0	4.59	77.5	0	Baton Rouge	Mississippi	77.5
Crops	1201	351.65	18	1	1	1	3.53	600	500.25	Baton Rouge	Mississippi	99.75
Crops	1202	357.63	18	1	0	0	4.47	1330.25	1250.25	Baton Rouge	Mississippi	80
Crops	1203	385.20	12	2	0	0	9.51	1290.75	1250.25	Baton Rouge	Mississippi	40.5
Crops	1204	381.58	12	2	0	0	8.39	1295.75	1250.25	Baton Rouge	Mississippi	45.5
Crops	1205	365.67	12	2	0	0	9.56	1288.5	1250.25	Baton Rouge	Mississippi	38.25
Crops	1206	373.50	12	2	0	0	8.79	2542.75	2500.25	Baton Rouge	Mississippi	42.5
Crops	1207	378.67	6	3	1	1	10.23	2537.25	2500.25	Baton Rouge	Mississippi	37
Crops	1208	356.15	6	3	1	1	10.32	2534.75	2500.25	Baton Rouge	Mississippi	34.5
Crops	1209	358.96	6	3	0	0	11.22	2532.25	2500.25	Baton Rouge	Mississippi	32
Crops	1210	357.34	6	3	0	0	10.51	4534.25	4500.25	Baton Rouge	Mississippi	34
Crops	1211	348.94	6	3	0	0	10.34	4534	4500.25	Baton Rouge	Mississippi	33.75
Crops	1212	363.40	6	3	0	0	11.82	4531	4500.25	Baton Rouge	Mississippi	30.75
Crops	1213	355.53	6	3	0	0	11.75	4530.5	4500.25	Baton Rouge	Mississippi	30.25
Crops	1214	366.00	6	3	1	0.5	10.84	6034	6000.25	Baton Rouge	Mississippi	33.75
Crops	1407	379.89	12	2	0	0	8.17	59.25	12.75	Mississippi	Baton Rouge	46.5

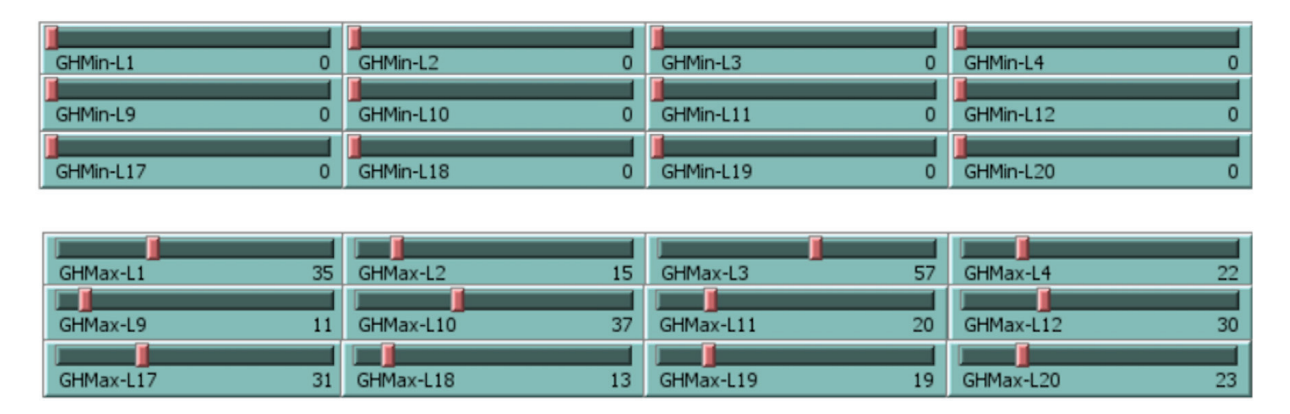


Fig. 11. Water level thresholds set by user for all sites to control extreme events criteria.

Table 9
Detailed outputs for trucks.

Detailed	outputs for truc	ks.						
ID	Product type	Distance traveled (miles)	Start time (ticks)	End time (ticks)	From	То	Time elapsed (ticks)	Avg. speed (mph)
5000	Petroleum	524.7424833	103	110.75	Fort Smith	Е	7.75	67.71
5001	Petroleum	524.5594318	103	111.25	Fort Smith	E	8.25	63.58
5002	Petroleum	524.5952797	103	110.25	Fort Smith	E	7.25	72.36
5003	Petroleum	524.3400126	103	110.25	Fort Smith	E	7.25	72.32
5004	Petroleum	524.3189491	103	110.5	Fort Smith	E	7.5	69.91
5005	Petroleum	525.4226671	103	110.5	Fort Smith	E	7.5	70.06
5006	Petroleum	524.7314365	103	110	Fort Smith	E	7	74.96
5007	Petroleum	524.2494159	103	110.25	Fort Smith	E	7.25	72.31
5008	Petroleum	524.4084918	103	110	Fort Smith	E	7	74.92
5009	Petroleum	524.5227015	103	110.25	Fort Smith	E	7.25	72.35
5010	Petroleum	524.5717312	103	110.5	Fort Smith	E	7.5	69.94
5011	Petroleum	524.3143702	103	109.75	Fort Smith	E	6.75	77.68
5012	Petroleum	524.2374395	103	110.5	Fort Smith	E	7.5	69.90
5013	Petroleum	524.1374195	103	110.25	Fort Smith	E	7.25	72.29
5014	Petroleum	524.6757786	103	110.25	Fort Smith	E	7.25	72.37
5015	Petroleum	524.2429046	103	110	Fort Smith	E	7	74.89
5016	Petroleum	167.7360173	103	105.5	Fort Smith	N	2.5	67.09
5017	Petroleum	177.1946809	103	105.5	Fort Smith	N	2.5	70.88
5018	Petroleum	443.1499304	103	109.75	Fort Smith	S	6.75	65.65
5019	Petroleum	450.1915388	103	109.5	Fort Smith	S	6.5	69.26
7000	Petroleum	242.3998382	142.5	146.5	Helena	E	4	60.60
7001	Petroleum	239.7554172	142.5	146	Helena	E	3.5	68.50
7002	Petroleum	243.9796093	142.5	146.5	Helena	E	4	60.99
7003	Petroleum	240.2386683	142.5	145.75	Helena	E	3.25	73.92
7004	Petroleum	241.5537637	142.5	146	Helena	E	3.5	69.02
7005	Petroleum	239.2439371	142.5	146.25	Helena	E	3.75	63.80
7006	Petroleum	240.4777264	142.5	145.75	Helena	E	3.25	73.99
7007	Petroleum	241.2591156	142.5	146.25	Helena	E	3.75	64.34
7008	Petroleum	241.0668822	142.5	146.25	Helena	E	3.75	64.28
7009	Petroleum	242.7985141	142.5	146.25	Helena	E	3.75	64.75
7010	Petroleum	241.4463379	142.5	146.25	Helena	E	3.75	64.39
7011	Petroleum	239.9652814	142.5	146	Helena	E	3.5	68.56
7012	Petroleum	243.0676827	142.5	146.25	Helena	E	3.75	64.82
7013	Petroleum	243.2426233	142.5	146.5	Helena	E	4	60.81
7014	Petroleum	238.8765655	142.5	145.75	Helena	E	3.25	73.50
7015	Petroleum	239.9229721	142.5	146	Helena	E	3.5	68.55
7016	Petroleum	394.0866412	142.5	148.5	Helena	N	6	65.68
7017	Petroleum	386.0744743	142.5	147.75	Helena	N	5.25	73.54
7018	Petroleum	262.8503073	142.5	147	Helena	S	4.5	58.41
7019	Petroleum	258.4577559	142.5	147	Helena	S	4.5	57.44
8000	Crops	240.4638423	47	50.5	Helena	E	3.5	68.70
8001	Crops	385.549631	47	52.75	Helena	N	5.75	67.05
8002	Crops	258.635328	47	50.5	Helena	S	3.5	73.90
8003	Crops	241.2157411	52.75	56.25	Helena	E	3.5	68.92
8004	Crops	385.151909	52.75	58	Helena	N	5.25	73.36
8005	Crops	258.5213772	52.75	57.25	Helena	S	4.5	57.45

(continued on next page)

Table 9 (continued).

ID	Product type	Distance traveled (miles)	Start time (ticks)	End time (ticks)	From	То	Time elapsed (ticks)	Avg. speed (mph)
8006	Crops	239.7437967	1021.25	1025	Helena	E	3.75	63.93
8007	Crops	384.7920906	1021.25	1026.75	Helena	N	5.5	69.96
8008	Crops	263.6299675	1021.25	1025	Helena	S	3.75	70.30
8009	Crops	240.3038144	1026.75	1030.5	Helena	E	3.75	64.08
8010	Crops	391.4770111	1026.75	1032.75	Helena	N	6	65.25
8011	Crops	255.6389391	1026.75	1031.25	Helena	S	4.5	56.81
8012	Crops	239.9652814	1032.75	1036.5	Helena	E	3.75	63.99
8013	Crops	388.9339639	1032.75	1038.75	Helena	N	6	64.82
8014	Crops	259.789386	1032.75	1036.25	Helena	S	3.5	74.23
8015	Crops	242.9573568	1038.75	1042.25	Helena	E	3.5	69.42
8016	Crops	383.1177057	1038.75	1044.25	Helena	N	5.5	69.66
8017	Crops	255.8213064	1038.75	1043.5	Helena	S	4.75	53.86
8018	Crops	242.8259393	1044.25	1047.5	Helena	E	3.25	74.72
8019	Crops	390.222719	1044.25	1049.5	Helena	N	5.25	74.33
8020	Crops	262.4966935	1044.25	1049	Helena	S	4.75	55.26
8021	Crops	242.2872164	1049.5	1053	Helena	E	3.5	69.22
8022	Crops	389.1117699	1049.5	1055.75	Helena	N	6.25	62.26
8023	Crops	253.3064752	1049.5	1053.5	Helena	S	4	63.33
8024	Crops	242.9258206	1056	1059.5	Helena	E	3.5	69.41
8025	Crops	392.8540749	1056	1061.5	Helena	N	5.5	71.43
8026	Crops	259.0699308	1056	1060.5	Helena	S	4.5	57.57
8027	Crops	242.0606581	1061.5	1064.75	Helena	E	3.25	74.48
8028	Crops	380.523792	1061.5	1067	Helena	N	5.5	69.19
8029	Crops	259.2975286	1061.5	1065.25	Helena	S	3.75	69.15
8030	Crops	242.3815963	2020.75	2024.25	Helena	E	3.5	69.25
8031	Crops	386.7121652	2020.75	2025.75	Helena	N	5	77.34
8032	Crops	257.3860023	2020.75	2025.25	Helena	S	4.5	57.20
8033	Crops	243.0613488	2025.75	2029.25	Helena	E	3.5	69.45
8034	Crops	384.1817111	2025.75	2031	Helena	N	5.25	73.18
8035	Crops	258.8727207	2025.75	2030.25	Helena	S	4.5	57.53
8036	Crops	242.2048536	2031	2034.75	Helena	E	3.75	64.59
8037	Crops	394.453156	2031	2037.25	Helena	N	6.25	63.11
8038	Crops	253.9643062	2031	2035.5	Helena	S	4.5	56.44
8039	Crops	243.3186303	2037.25	2040.5	Helena	E	3.25	74.87
8040	Crops	388.3791161	2037.25	2042.5	Helena	N	5.25	73.98
8041	Crops	258.4626828	2037.25	2041	Helena	S	3.75	68.92
8042	Crops	241.4879116	2042.5	2046.25	Helena	E	3.75	64.40
8043	Crops	385.1115147	2042.5	2047.75	Helena	N	5.25	73.35
8044	Crops	264.8154224	2042.5	2047	Helena	S	4.5	58.85
8045	Crops	241.4091439	2047.75	2051.25	Helena	E	3.5	68.97
8046	Crops	390.574694	2047.75	2053	Helena	N	5.25	74.40
8047	Crops	254.1111329	2047.75	2052.25	Helena	S	4.5	56.47

CRediT authorship contribution statement

José Azucena: Conceptualization, Methodology, Software, Simulation, Writing . Basem Alkhaleel: Conceptualization, Methodology, Formal analysis, Writing . Haitao Liao: Conceptualization, Methodology, Writing - review & editing, Project administration. Heather Nachtmann: Methodology, Writing - review & editing, Project administration.

Acknowledgments

Funding: This work was supported by the U.S. National Science Foundation [Grant No. CMMI–1745353]. The authors would also like to thank MarTREC at the University of Arkansas for hosting the website for the dissemination of this simulation tool.

Appendix. Introduction to the developed simulation tool

Simulation setup

A user can use model controls (Figs. 3–4) to quickly adjust the settings of the initial environment (see buttons, sliders, and other controls). To initiate a simulation run after setting up the environment, the user can input various attributes through sliders, choosers, and switches. The steps are as follows:

Step 1: First, click the "Spatial Temporal Analysis" button to run the spatio-temporal model to generate predicted GH and lock availability data.

- **Step 2:** Click the "Setup Environment" button. This button is used to initialize the model, and it is a NetLogo "once-button" that runs its code once. After this step, all maps will be drawn on the user interface.
- Step 3: Click the "Add Ports" button to draw eight circles on the waterways that depict the ports of interest in our model.
- **Step 4:** Click the "Add Locks & Sites" button to initialize and draw all fifteen locks and twenty-four sites with their variables. Then, click "Add Vessels" to draw vessels on the ports based on the data. The vessels are categorized according to their size and speed into three groups, and they carry two types of products in the current setting: petroleum and crops.

After completing the above steps, a value for "Simulation-Time" needs to be set to indicate the number of months the simulation will run. The available options are 3, 6, 9, and 12 months. "Fleet-Size" provides the number of trucks required to carry products from one vessel through the highways when vessels reach to their destinations, and when they are unable to move for a certain amount of time due to extreme events. The global slider "GH-Threshold" may need to be adjusted to a reasonable value (higher than the individual sites' GHs which also can be adjusted as shown in Fig. 11). This value acts as the threshold value of GH, which is being compared with the hourly value of GH at each site. Such information about GH thresholds can be adopted from sources such as the United States Geological Survey (USGS) [46]. We can change the value at runtime. There are fifteen switches, each of which acts as a controller to turn on/off the corresponding lock. The selection can also be changed during the runtime. When one lock is closed, the vessels that are supposed to pass through the lock will wait in the previous node in the path and will not move forward until the lock is reopened. If the "LockRandomFailures" button is set to "On", locks' failure and repair events will be generated using random variates. The mean time to these events is controlled by the parameters "AvgTimeToLockFail" and "AvgTimeToLockRepair". After all the settings are completed, click the "Start Simulation" button xand the vessels at each port start moving towards their predefined destinations. Each vessel checks for any unsafe circumstances at the locks and sites along its route and makes decisions accordingly.

Model outputs

After running the simulation tool, multiple numerical outputs are generated for the user. The outputs can be classified into summaries and detailed results. The summaries are shown in Tables 4-7 and Figs. 7-9. As mentioned in Section 4.2, Tables 4 and 7 show summary statistics for the vessels traveled between every two ports classified by the vessel category. In addition, summarized vessel and truck tables such as Table 4 show the number of vessels (trucks) that have traveled from ports, average speed of travel, product type carried and other statistics that help the user understand the commodity flow changes under each scenario. Each summarized table output is exported as a "CSV" file format that can be used as an input file to other statistical software or programming languages for further analysis. Furthermore, some of these statistical summaries are plotted using the NetLogo R extension and exported as publication-quality "PDF" files such as the ones shown in Figs. 7-9. The outputs of the simulation tool also include detailed information about all vessels appeared in the model (see Table 8). Like the records mentioned before, the detailed information includes the product type carried, category of the vessel, total weight of the product, and a defined ID for each vessel (modeled as a turtle). Also registered, each vessel's start time, time of departure from its origin, and its end time (time of arrival at its destination). These records can help extend the simulation analysis and contribute to the model's debugging and validation. These results are tabulated and exported as a "CSV" file with additional detailed information about the trucks, as shown in Table 9. The detailed information in Table 9 is useful to identify individual trucks by their ID, destination, departure (start) and arrival (end) times in the simulation along with distance traveled in miles and average speed in mph for each truck. Such information becomes useful in analyzing a given product's current logistic plan and finding possible ways to alter and improve the current one.

References

- [1] J. Ellis, D. Fisher, T. Longstaff, L. Pesante, R. Pethia, Report to the President's Commission on Critical Infrastructure Protection, Technical Report, Defense Technical Information Center, 1997, http://dx.doi.org/10.21236/ada324232.
- [2] US Department of Transportation, Geospatial at the bureau of transportation statistics, Washington, DC, 2017, available via https://maps.bts.dot.gov/arcgis/home/index.html.
- $[3] \begin{tabular}{ll} US Army Corps of Engineers, US army corps of engineers: Navigation data center, 2020, available via $$http://www.navigationdatacenter.us/. $$$
- [4] T. Bipasha, J. Azucena, B. Alkhaleel, H. Liao, H. Nachtmann, Hybrid simulation to support interdependence modeling of a multimodal transportation network, in: 2019 Winter Simulation Conference, WSC, IEEE, National Harbor, MD, 2019, pp. 1390–1401, http://dx.doi.org/10.1109/WSC40007.2019. 9004813
- [5] R. Pant, K. Barker, T.L. Landers, Dynamic impacts of commodity flow disruptions in inland waterway networks, Comput. Ind. Eng. 89 (2015) 137-149.
- [6] P.R. Herr, Approaches to Mitigate Freight Congestion, Vol. 287, Technical Report, United States Government Accountability Office, Washington, DC, 2008, p. 12.
- [7] Freight Research, National cooperative freight research program: Current and completed projects, Transp. Res. Board (2010).
- [8] US Department of Transportation, Freight facts and figures 2009, Technical Report, Federal Highway Administration, Office of Freight Management and Operations, Washington, DC., 2009, p. 274.
- [9] Cambridge Systematics Inc., National Rail Freight Infrastructure Capacity and Investment Study, Technical Report, Cambridge, MA, 2007.
- [10] US Department of Transportation. Maritime Administration, America's Marine Highway Report to Congress. Technical Report, Washington, DC, April, 2011.
- [11] J. Schweighofer, The impact of extreme weather and climate change on inland waterway transport, Nat. Hazards 72 (1) (2014) 23-40.
- [12] S.-L. Wang, P. Schonfeld, Scheduling interdependent waterway projects through simulation and genetic optimization, J. Waterway Port Coast. Ocean Eng. 131 (3) (2005) 89–97.
- [13] J.L. Carroll, M.S. Bronzini, Waterway transportation simulation models: Development and application, Water Resour. Res. 9 (1) (1973) 51-63.
- [14] Y. Triska, E.M. Frazzon, V.M.D. Silva, Proposition of a simulation-based method for port capacity assessment and expansion planning, Simul. Model. Pract. Theory 103 (2020) 102098.

- [15] R. Larson, A. Minkofft, P. Gregory, A computer simulation model for fleet sizing for the marine division of the New York City department of sanitation, Waste Manag. Res. 9 (4) (1991) 267–276, http://dx.doi.org/10.1016/0734-242x(91)90017-2.
- [16] J. Swedish, Simulation of an inland waterway barge fleet distribution network, in: 1998 Winter Simulation Conference. Proceedings (Cat. No.98CH36274), Vol. 2, IEEE, Washington, DC, 1998, pp. 1219–1221, http://dx.doi.org/10.1109/wsc.1998.745982.
- [17] G.D. Taylor, T.C. Whyte, G.W. DePuy, D. Drosos, A simulation-based software system for barge dispatching and boat assignment in inland waterways, Simul. Model. Pract. Theory 13 (7) (2005) 550–565.
- [18] F. Oztanriseven, H. Nachtmann, Economic impact analysis of inland waterway disruption response, Eng. Econ. 62 (1) (2017) 73-89.
- [19] G. Desquesnes, D. Alves, E. Duviella, G. Lozenguez, A. Doniec, Simulation architecture based on distributive MDP for inland waterway management, in: G.L. Loggia, G. Freni, V. Puleo, M.D. Marchis (Eds.), HIC 2018. 13th International Conference on Hydroinformatics, in: EPiC Series in Engineering, vol. 3, EasyChair, 2018, pp. 555–563, http://dx.doi.org/10.29007/fbmt.
- [20] M. Ouyang, Review on modeling and simulation of interdependent critical infrastructure systems, Reliab. Eng. Syst. Saf. 121 (2014) 43-60.
- [21] C.W. Howe, J.L. Carroll, A.P. Hurter Jr, W.J. Leininger, S.G. Ramsey, N.L. Schwartz, E. Silberberg, R.M. Steinberg, Inland Waterway Transportation: Studies in Public and Private Management and Investment Decisions, Johns Hopkins, Baltimore, 1969.
- [22] M.D. Dai, Delay Estimation on Congested Waterways (Ph.D. thesis), 1991, p. 146, ProQuest Dissertations and Theses.
- [23] C.-J. Ting, P. Schonfeld, Optimization through simulation of waterway transportation investments, Transp. Res. Rec.: J. Transp. Res. Board 1620 (1) (1998) 11–16.
- [24] M. Ouyang, L. Hong, Z.-J. Mao, M.-H. Yu, F. Qi, A methodological approach to analyze vulnerability of interdependent infrastructures, Simul. Model. Pract. Theory 17 (5) (2009) 817–828.
- [25] A. Bush, W. Biles, G. DePuy, Iterative optimization and simulation of barge traffic on an inland waterway, in: Proceedings of the 2003 International Conference on Machine Learning and Cybernetics (IEEE Cat. No.03EX693), Winter Simulation Conference, IEEE, Piscataway, New Jersey, 2004, pp. 1751–1756.
- [26] W. Biles, D. Sasso, J. Bilbrey, Integration of simulation and geographic information systems: Modeling traffic flow on inland waterways, in: Proceedings of the 2004 Winter Simulation Conference, 2004, IEEE, 2005, pp. 331–337, http://dx.doi.org/10.1109/wsc.2004.1371477.
- [27] C. Colon, S. Hallegatte, J. Rozenberg, Transportation and Supply Chain Resilience in the United Republic of Tanzania, World Bank, 2019, http://dx.doi.org/10.1596/31909.
- [28] J. Verschuur, E. Koks, J. Hall, Port disruptions due to natural disasters: Insights into port and logistics resilience, Transp. Res. D 85 (2020) 102393.
- [29] W. Zhu, K. Liu, M. Wang, E.E. Koks, Seismic risk assessment of the railway network of China's mainland, Int. J. Disaster Risk Sci. 11 (4) (2020) 452-465.
- [30] N.A.C. Cressie, C.K. Wikle, Statistics for Spatio-Temporal Data, Wiley, Hoboken, N.J, 2011, p. 624.
- [31] P.C. Kyriakidis, A.G. Journel, Geostatistical space-time models: A review, Math. Geol. 31 (6) (1999) 651-684.
- [32] HSIP, Homeland security infrastructure program (HSIP) data, 2019, available via https://hifld-dhs-gii.opendata.arcgis.com/.
- [33] HIFLD, Homeland infrastructure foundation-level data (HIFLD), 2020, available via https://hifld-dhs-gii.opendata.arcgis.com/datasets?q=*dam&sort_by=relevance.
- [34] HIFLD, Homeland infrastructure foundation-level data (HIFLD), 2020, available via https://data.navigationdatacenter.us/Locks/Public-Lock-Unavailability-Detailed-Report/p3mn-gzqj.
- [35] HIFLD, Homeland infrastructure foundation-level data (HIFLD), 2020, available via https://hifld-dhs-gii.opendata.arcgis.com/datasets?q=flood.
- [36] NOAA, National oceanic and atmospheric administration (NOAA climate), 2020, available via https://www.noaa.gov/climate.
- [37] MarTREC, Maritime transportation research and transportation center, 2020, available via https://martrec.uark.edu/.
- [38] MarTREC, Maritime Transportation Resource Data Bank- MarTREC, University of Arkansas, 2020, available via https://martrec.uark.edu/research/resource-data-bank.php.
- [39] MarTREC Simulation Tool, Data simulation to support interdependence modeling of a multimodal transportation network, 2020, available via https://martrec.uark.edu/data/index.php.
- [40] K.S. Bakar, S.K. Sahu, et al., spTimer: Spatio-temporal bayesian modelling using R, J. Stat. Softw. 63 (15) (2015) 1–32.
- [41] B. Matérn, Spatial Variation, Springer-Verlag, New York, 1986, p. 153.
- [42] U. Wilensky, NetLogo, Center for Connected Learning and Computer-Based Modeling, Northwestern University, Evanston, IL, 1999, available via https://ccl.northwestern.edu/netlogo/.
- [43] S. Tisue, U. Wilensky, NetLogo: Design and implementation of a multi-agent modeling environment, in: Proceedings of the Agent 2004 Conference on Social Dynamics: Interaction, Reflexivity and Emergence, Chicago, IL, 2004, pp. 7–9.
- [44] H. Nachtmann, K.N. Mitchell, C.E. Rainwater, R. Gedik, E.A. Pohl, Optimal dredge fleet scheduling within environmental work windows, Transp. Res. Rec. 2426 (1) (2014) 11 19
- [45] National Weather Service, Advanced hydrologic prediction service, 2020, available via https://water.weather.gov/ahps2/hydrograph.php?wfo=fsd&gage=lnni4.
- [46] United States Geological Survey, USGS surface-water data for the nation, 2020, available via https://waterdata.usgs.gov/nwis/sw.